



Study on morphologies of Co microcrystals produced by solvothermal method with different solvents

Lianfeng Duan, Shusheng Jia, Lijun Zhao*

Key Laboratory of Automobile Materials (Jilin University), Ministry of Education and Department of Materials Science and Engineering, Jilin University, Renmin Street No. 5988, Changchun 130022, PR China

ARTICLE INFO

Article history:

Received 25 June 2009

Received in revised form 8 November 2009

Accepted 4 January 2010

Available online 11 January 2010

Keywords:

- A. Magnetic materials
- B. Chemical synthesis
- B. Crystal growth
- D. Microstructure
- E. Magnetic properties

ABSTRACT

Cobalt microcrystals with different sizes and morphologies were fabricated via a facile solvothermal method. The effects of different solvents on the sizes and morphologies are investigated separately. Flowerlike cobalt with around tens of microns in diameter is obtained in ethanol. Meanwhile, of microdisks and octadecahedra with the edge lengths about several microns are fabricated in ethylene glycol and glycerol, respectively. Reduction potential and viscosity rank of the solvents play the important roles in controlling the sizes and morphologies of cobalt. Moreover, room-temperature magnetic measurement shows that the magnetic properties of cobalt microcrystals depend on their morphologies.

© 2010 Elsevier Ltd. All rights reserved.

1. Introduction

In recent years, much attention has been focused on the fabrication of nanoscale and microscale crystals. Ferromagnetic cobalt (Co) has received considerable attention both theoretically and experimentally due to its extraordinary electrical, catalytic, and magnetic properties, which are of interest for basic scientific research and potential technological applications, for example, catalysis, electronics, high-density magnetic recording media, sensors, biotechnology, and biomedical nanotechnology catalysts, artificial cells, coatings, etc. [1–9]. The size, morphology, and structure of materials significantly influence their physical and chemical properties, and therefore their technological applications [10]. Up to now, various morphologies of ferromagnetic cobalt crystals such as wires, rods, disks, rings and spheres have been successfully fabricated [11–15]. Diverse synthetic methodologies, such as the thermal decomposition of cobalt carbonyl, organometallic precursors, template-mediated synthesis, solvothermal, and the ultrasonic spray pyrolysis methods, have also been proposed and demonstrated to prepare cobalt particles [16–20]. In particular, solvothermal method demonstrates its superiority in controlling the shapes of crystals [13,21,22].

Co is an important ferromagnetic metal, which can crystallize in three structures: the hexagonal-close-packed (hcp), the face-

centered cubic (fcc) and the epsilon phases. Generally, the hcp phase with a high coercivity is of interest in the field of permanent magnets, while the fcc phase with a low coercivity can be used as soft-magnetic materials [23]. The structure, size, and shape play an important role in defining the properties of the particles as well as their use in practical applications. Various morphologies of Co microcrystals with hcp structure were fabricated by solvothermal method. In addition, the effects of different solvents on the morphologies of cobalt microcrystals are discussed. Herein, the metallic Co microcrystals with different morphologies and sizes were synthesized by solvothermal method using three kinds of solvents. To investigate the effect of microstructure on the magnetic properties, we also studied the magnetic properties of the Co microcrystals with various morphologies.

2. Experimental

All reagents were commercial products with analytical grade without further purification. In a typical procedure, 0.5 g of $\text{CoCl}_2 \cdot 6\text{H}_2\text{O}$ was first dissolved in 20 mL of ethanol (S1), ethylene glycol (S2) or glycerol (S3) under magnetic stirring at room temperature. The solution was intensively stirred for 20 min, then 1.0 mL of ethylenediamine (EDA) and 1.0 mL hydrazine monohydrate $\text{N}_2\text{H}_4 \cdot \text{H}_2\text{O}$ (55 vol.% analytical reagent) were added dropwise to the solution at room temperature by vigorous stirring for 20 min. Subsequently, the solution was transferred into a 30 mL Teflon-lined stainless steel autoclave. The autoclave was sealed and maintained at 200 °C for 24 h and then cooled to room temperature naturally.

* Corresponding author. Tel.: +86 431 85095878; fax: +86 431 85095876.
E-mail addresses: lijunzhao@jlu.edu.cn, nokiaxf99@yahoo.com.cn (L. Zhao).

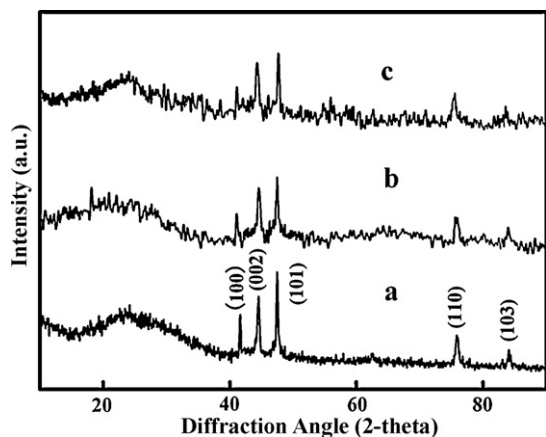


Fig. 1. XRD patterns of the as-obtained products (a) S1, (b) S2, and (c) S3.

The products (S1, S2, and S3) were filtered off, washed several times with distilled water and absolute ethanol, and finally dried in a vacuum oven at 60 °C for 4 h.

The phases were identified by means of X-ray diffraction (XRD) with a Rigaku D/max 2500pc X-ray diffractometer with Cu K α radiation (λ) 1.54156 (Å) at a scan rate of 0.04° s⁻¹. The morphologies were characterized by a JEOL JSM-6700F field-emission scanning electron microscopy (FESEM) operated at an acceleration voltage of 5.0 kV. Transmission electron microscopy (TEM) and high-resolution TEM (HRTEM) observations were carried out on a JEOL 2100F with an emission voltage of 200 kV. Magnetic measurements were carried out using a Quantum Design superconducting quantum interference device (SQUID) magnetometer (LakeShore 7307).

3. Results and discussion

Fig. 1 gives XRD patterns of the as-prepared cobalt crystals. All of them are well crystallized. The diffraction peaks for the samples could be indexed to pure hexagonal-close-packed (hcp) cobalt phase (JCPDS 05-0727), and no impurities can be detected.

The morphologies of the samples were observed by FESEM. Fig. 2a is a typical low-magnification SEM image of S1, from which we can find that flowerlike shapes are the exclusive products, which means that the flowerlike cobalt can be prepared in large scale. A high-magnification SEM image of S1 (Fig. 2b) shows that flowerlike cobalt microcrystals with about 30 μ m in diameter. Furthermore, the rough surfaces of S1 confirmed that flowerlike shapes consisted of small particles stacked in a random fashion.

SEM image of S2 (Fig. 3a) displays that the product is composed of 2–3 μ m-thick and 1.5–2 μ m-wide prism-like crystals. Fig. 3b is the SEM image of S3, which shows that the thickness of the octadecahedra is about 2.5 μ m, and their width is 1.5–2 μ m. The special shapes obtained from the solvothermal process, which means that the polyols may serve as stabilizing reagents to bind the surfaces of cobalt microcrystals. Furthermore, this serves as an evidence that the polyols can slow down the growth ratio of the cobalt crystals, because the dissolution–crystallization process of the precursor is inhibited.

Further insight into the morphology and microstructure of S3 was gained using TEM and HRTEM. The HRTEM and SAED were performed in the region of polyhedra as labeled in Fig. 4a which is the TEM image of S3. The SAED pattern (Fig. 4b) exhibits the good crystallization of cobalt microcrystals. Furthermore, the SAED spots can be steadily indexed to (1 0 1), (1 0 3), (0 0 2) facets which is in good agreement with the XRD data. The lattice fringes of crystalline S3 can be seen clearly from Fig. 4c, and the interplanar spacing was measured to be 0.20 nm, corresponding to the (0 0 2) planar spacing of hcp cobalt. The (0 0 2) plane of hcp-Co

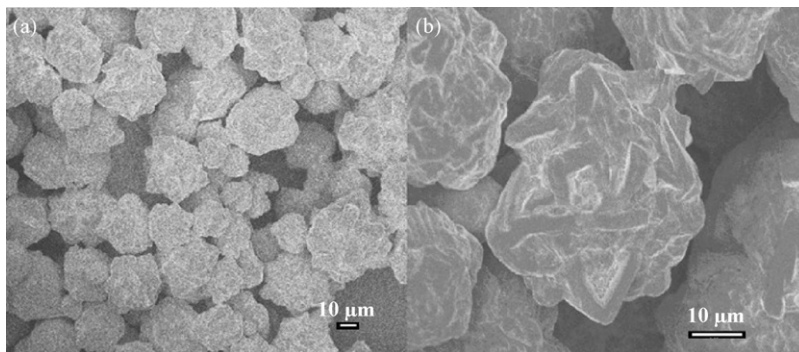


Fig. 2. SEM image of S1 (a) low magnification and (b) high magnification.

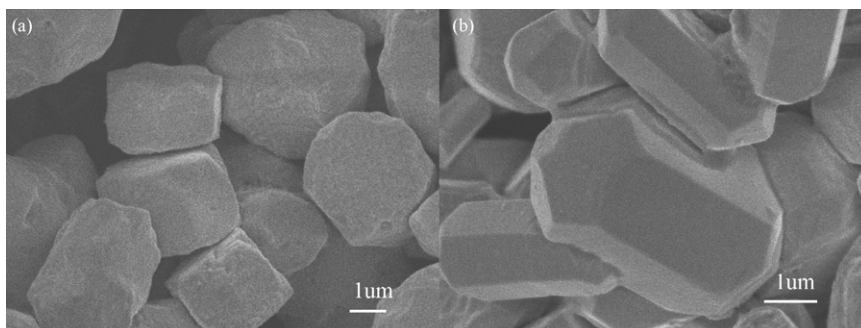


Fig. 3. SEM images of Co microcrystal (a) S2 and (b) S3.

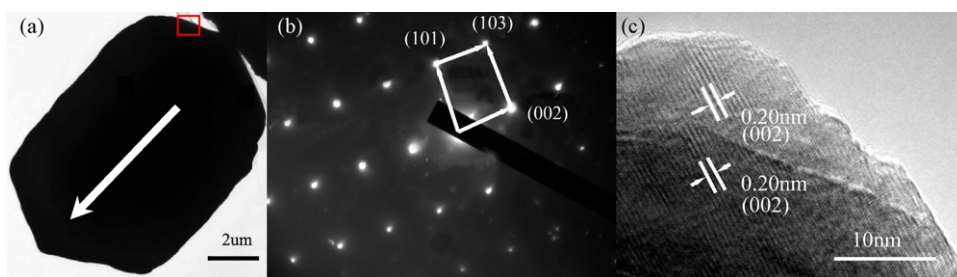


Fig. 4. (a) TEM, (b) SAED, and (c) HRTEM images of S3.

corresponds to the $[0\ 0\ 2]$ direction which is parallel to the growth direction as the arrow shown in Fig. 4a.

Murphy [24] had claimed that the preferential adsorption of molecules and ions in solution onto different crystal facets directs the growth of particles into various shapes by controlling the growth rates along different crystal axes. In the ethylene glycol or glycerol, EDA may play a role to direct the growth of cobalt crystals, because of the interaction between the $-\text{NH}_2$ and the cobalt ions or the $-\text{NH}_2$ selective adsorption on the particle surfaces. Experimental observations suggest that steric interactions among neighboring adsorbed molecules may have an impact on the growth rate of the $(0\ 0\ 2)$ plane [13]. Moreover, the addition of $\text{N}_2\text{H}_4 \cdot \text{H}_2\text{O}$ could improve the yields of cobalt powders.

To shed light on the possible growth processes of the Co microcrystals with various morphologies under different solvents, schematic illustration was drawn in Fig. 5. It is known that the physical and chemical properties of the solvents can influence the solubility, reactivity, and diffusion behavior of the reagents, and even influence the growth of morphologies of products. On the one hand, the sequence of boiling point of the three kinds of solvents from low to high is ethanol, ethylene glycol, and glycerol. On the other hand, the viscosity ranking of the three kinds of solvents is ethanol < ethylene glycol < glycerol. Furthermore, hydroxyl numbers of the polyols decide the reducing abilities of the three kinds of solvents. To the ethanol, its lower boiling point leads to the highest pressure in the closed reaction systems at the same reaction temperature, which facilitates the growth of cobalt particles; its lower viscosity helps the quicker nucleation. When the concentration of growth species reduces below the minimum concentration for nucleation, nucleation stops, whereas the growth continues until the equilibrium concentration of the precipitated species is reached. At this stage, kinetic control and focus of size occurs: the smaller particles grow more rapidly than the larger ones, because the free energy driving force is larger for smaller particles than for larger ones, if the particles are slightly larger than

the critical size. By taking advantage of this key feature, nearly monodisperse size distribution can be obtained at this stage by either stopping the reaction (nucleation and growth) quickly or by supplying a reactant source to keep a saturated condition during the reaction. The driving force for this spontaneous oriented attachment is that the elimination of the pairs of high energy surfaces will lead to a substantial reduction in the surface free energy from the thermodynamic viewpoint [25]. Because of the quick nucleation and easy growth in the ethanol solution, EDA has few effects on the crystal planes. The elimination of the pairs of crystal planes is random. Hence, the flowerlike morphologies of cobalt microcrystals are prepared in the ethanol solution by further crystallization. Moreover, the relatively low reduction ability for ethanol results in a slow reduction rate, which brings about the largest crystallite sizes for S1. In addition, the particle sizes can be controlled by reduction potential of the polyol (P_{redox}) [26]. The P_{redox} of the polyol is high, and then the size of the particles becomes smaller. In the present system, the P_{redox} of ethanol is much weaker than EG and Gly, so the particle sizes of S1 are larger than these of S2 and S3. To some extent, higher viscosity can slow down the growth rate and be more advantageous for the isotropic growth [27]. In the ethylene glycol or the glycerol solvent, the relatively slow nucleation and growth favor the selective adsorption of $-\text{NH}_2$ on the crystal planes of cobalt crystals, which are good for the formation of cobalt microdisks and octadecahedra. For the formation of microdisks, $-\text{NH}_2$ functions may bind strongly to $(0\ 0\ 1)$ surfaces of the growing Co crystallites. So the particles grow preferentially along the $[0\ 0\ 1]$ direction and the growth rate along the $[0\ 0\ 1]$ direction is much slower than that along the $[1\ 1\ 0]$ direction, leading to the formation of microdisks with the edge length and height of about 3 and 0.6 μm , respectively. For the formation of octadecahedra, $-\text{NH}_2$ may bind strongly to $(0\ 0\ 1)$ surface of the growing Co crystallites. So the particles grow along the $[0\ 0\ 1]$ is much faster than that along $[1\ 1\ 0]$ direction, causing the formation of octadecahedra; and the $(1\ 0\ 0)$ surfaces of S3 have

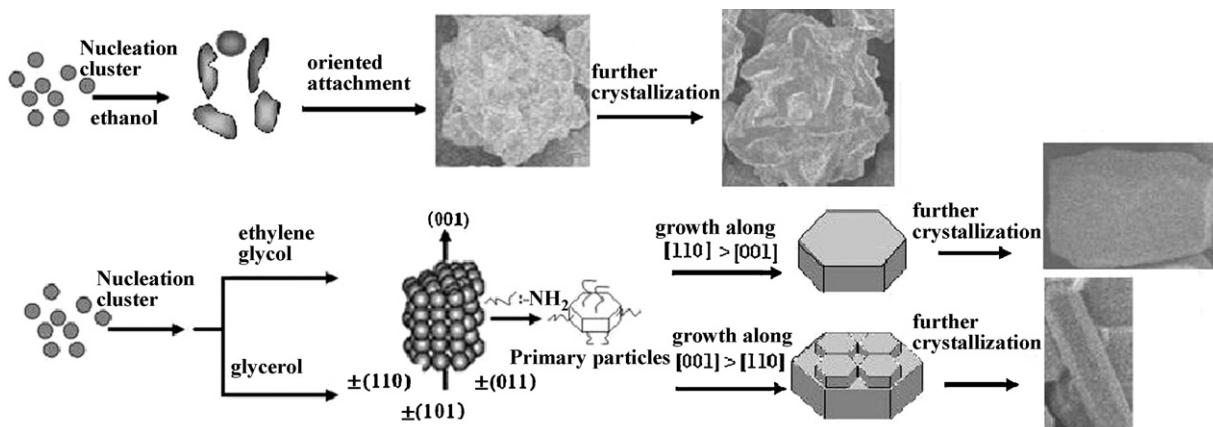


Fig. 5. Schematic illustration of the possible formation processes of the Co microcrystals with various morphologies under different solvents.

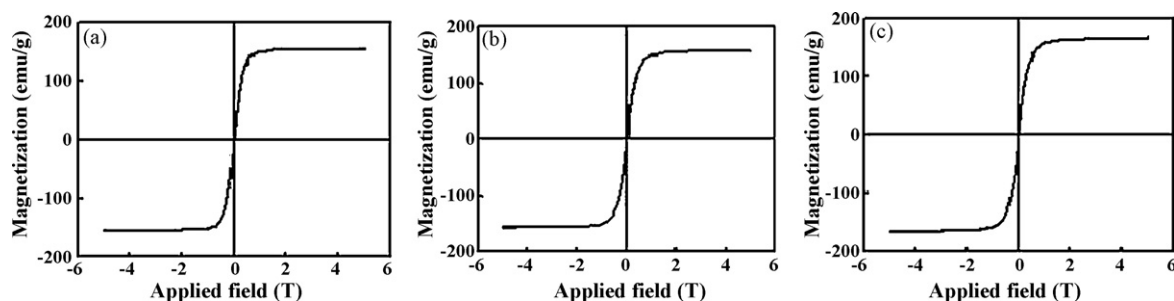


Fig. 6. The magnetization curve measured at room temperature for Co microcrystals (a) S1, (b) S2, and (c) S3.

an inclination to disappear. Optional attachment of the cobalt particles may happen in the ethanol solution; oriented attachment mechanism may explain the formation of cobalt microdisks and octadecahedra. With rotation of the adjacent particles, they share the same crystallographic orientation and subsequent coalescence. The regular aggregates are formed through the oriented attachment and self-assembly, which are similar to the report on formation of silver and Co by Fang and Zhu [28,29]. After the self-assembly process, the loose structures become compact gradually through further crystallization.

In order to investigate the influence of morphologies on the magnetic properties, the magnetic measurement for the Co microcrystals is performed. The room-temperature hysteresis loops of S1, S2, and S3 are shown in Fig. 6. Furthermore, the magnetic parameters obtained from Fig. 6 are listed in Table 1. To S1, S2, and S3, the values of saturation magnetization (M_s) are 156, 159, and 165 emu/g, respectively. The values of remnant magnetization (M_r) are 1.4, 2.9, and 4.3 emu/g; the values of coercivity (H_c) are 24, 44, and 77 Oe. It is generally accepted that when the particle sizes are larger than the single domain region, the values of M_s and M_r are increased with the increase of particle sizes. However, different phenomenon is observed from our experimental results. The use of various solvents during the solvothermal process may be responsible for the different results comparing with the above mention. For S1, it has the lowest values of M_s , M_r , and H_c . For S3, it owns the highest values of M_s , M_r , and H_c . Especially, the values of H_c for the samples are different from that of spherical cobalt particles (375 Oe) and the wire-like cobalt particles (389 Oe) [30]. Magnetization investigation confirms that the samples prepared by the solvothermal method using different solvents show relatively good soft magnetism.

Moreover, higher viscosity of solvent can slow down the growth rate and be more advantageous for the complete crystallization. Hence, the S3 possesses the highest M_s value. Besides, shape anisotropy might be responsible for the sequences of coercivity values for samples. It is well known that the particles with ellipse morphology had the lowest shape anisotropy. Therefore, we speculated that disks and octadecahedra had the higher shape anisotropy energy. Irregular flowerlike shape was close to ellipse, so they had the lowest coercivity value.

Table 1

Magnetic parameters obtained from hysteresis loops.

Samples	S1	S2	S3
M_s (emu/g)	156	159	165
M_r (emu/g)	1.4	2.9	4.3
H_c (Oe)	24	49	77

4. Conclusions

In summary, flowerlike, disk-shaped, and polyhedral Co microcrystals are prepared by the solvothermal method with different solvents. It has been found that the solvents affect the crystallite sizes and the morphologies of the Co microcrystals. Both the reduction potential and the viscosity ranking of the solvents play pivotal roles in controlling the sizes and the shapes of cobalt particles. Furthermore, the magnetic properties of cobalt microcrystals depend on their morphologies.

Acknowledgement

This work was supported by the Basic Research Expenses for the Special Funds of Jilin University.

References

- [1] D. Zhang, L. Qi, J. Ma, H. Cheng, *Adv. Mater.* 14 (2002) 1499–1502.
- [2] A.B. Bourlinos, M.A. Karakassides, D. Petridis, *Chem. Commun.* 16 (2001) 1518–1519.
- [3] Z. Zhong, Y. Yin, B. Gates, Y. Yia, *Adv. Mater.* 12 (2000) 206–209.
- [4] I. Lisiecki, *J. Phys. Chem. B* 109 (2005) 12231–12244.
- [5] M. Green, *Chem. Commun.* 24 (2005) 3002–3011.
- [6] Y. Liu, S.A. Majetich, R.D. Tilton, *Environ. Sci. Technol.* 39 (2005) 1338–1345.
- [7] D. Farrell, Y. Cheng, R.W. McCallum, *J. Phys. Chem. B* 109 (2005) 13409–13419.
- [8] B. Catherine, *J. Mater. Chem.* 15 (2005) 543–547.
- [9] Y.J. Song, M.M. Hartwig, *Chem. Mater.* 18 (2006) 2817–2827.
- [10] Y.W. Jun, J.S. Choi, J.W. Cheon, *Angew. Chem. Int. Ed.* 45 (2006) 3414–3439.
- [11] L. Vila, P.L. Vincent, D.D. Pra, *Nano Lett.* 4 (2004) 521–524.
- [12] F. Dumestre, B. Chaudret, C. Amiens, *Angew. Chem. Int. Ed.* 41 (2002) 4286–4289.
- [13] V.F. Puentes, D. Zanchet, C.K. Erdonmez, A.P. Alivisatos, *J. Am. Chem. Soc.* 124 (2002) 12874–12880.
- [14] S.L. Tripp, R.E. Dunin-Borkowski, A. Wei, *Angew. Chem Int. Ed.* 42 (2003) 5591–5593.
- [15] Y.J. Zhang, S. Ma, D. Li, Z.H. Wang, *Mater. Res. Bull.* 43 (2008) 1957–1965.
- [16] V.F. Puentes, K.M. Krishnan, A.P. Alivisatos, *Science* 291 (2001) 2115–2117.
- [17] F. Dumestre, B. Chaudret, C. Amiens, M. Respaud, P. Fejes, P. Renaud, P. Zurcher, *Angew. Chem. Int. Ed.* 42 (2003) 5213–5216.
- [18] M. Knez, A.M. Bittner, F. Boes, C. Wege, H. Jeske, E. Mai, K. Kern, *Nano Lett.* 3 (2003) 1079–1082.
- [19] H.L. Niu, Q.W. Chen, H.F. Zhu, Y.S. Lin, X. Zhang, *J. Mater. Chem.* 13 (2003) 1803–1805.
- [20] S. Gürmen, S. Stopic, B. Friedrich, *Mater. Res. Bull.* 41 (2006) 1882–1890.
- [21] L.J. Zhao, H.J. Zhang, J.K. Tang, S.Y. Song, F. Cao, *Mater. Lett.* 63 (2009) 307–309.
- [22] Q. Xie, Y.T. Qian, S.Y. Zhang, S.Q. Fu, W.C. Yu, *Eur. J. Inorg. Chem.* 12 (2006) 2454–2459.
- [23] D.P. Dinepa, M.G. Bawendi, *Angew. Chem. Int. Ed.* 38 (1999) 1788–1791.
- [24] C.J. Murphy, *Science* 298 (2002) 2139–2141.
- [25] Q. Zhang, S.-J. Liu, S.-H. Yu, *J. Mater. Chem.* 19 (2009) 191–207.
- [26] D. Kodama, K. Shinoda, K. Sato, *Adv. Mater.* 18 (2006) 3154–3159.
- [27] L.J. Zhao, H.J. Zhang, Y. Xing, *Chem. Mater.* 20 (2008) 198–204.
- [28] J. Fang, H. You, P. Kong, Y. Yi, X. Song, B. Ding, *Cryst. Growth Des.* 7 (2007) 864–867.
- [29] L.P. Zhu, H.M. Xiao, W.D. Zhang, *Cryst. Growth Des.* 8 (2008) 1113–1119.
- [30] H.L. Niu, Q.W. Chen, H.F. Zhu, Y.S. Lin, X.J. Zhang, *Mater. Chem.* 13 (2003) 1803–1805.